TADEUSZ KORONOWICZ,
Assoc.Prof.,D.Sc.,N.A.
JAN SZANTYR, Prof.,D.Sc.,N.A.
TOMASZ BUGALSKI, D.Sc.,N.A.
Polish Academy of Sciences
Institute of Fluid Flow Machinery, Gdańsk

Theoretical model for determining the pressure field resulting from hull flow and operation of the marine propeller

SUMMARY

In this paper theoretical background is presented of the computational model used to develop the computer program for determination of the pressure field connected with flow around the hull and operation of the ship propeller. A theoretical model of the potential flow around the hull moving with steady speed on the inflexible water surface over the flat sea bed is described, as well as a model for determination of the secondary wave system connected with the flexibility restoration of the surface. A computation model is also presented of the hull boundary layer assumed in the program, results of which are used to modifying the hull form (its enlargement by the displacement boundary layer thickness) and to determining the velocity field in the area of propeller operation.

A computation model of the propeller is also described, based on the deformable lifting surface theory adapted to analyzing the propeller performance within non-uniform velocity field behind the hull, with ability of detecting the cavitation and determining the pressure induced by it.

INTRODUCTION

If is vital to know the pressure field around such ships as naval, geophysic research, or fishing vessels because the high level of hydrodynamic pressure (a separate part of the pressure field with frequencies lower than 10 Hz) and acoustic pressure (a part of the field with frequencies higher than 10 Hz) makes proper functioning of the vessels impossible. In consequence many research centres are concerned with experimental and theoretical investigations of the problem. Difficulties connected with analytical determination of the acoustic pressure field result from a highly differentiated character of the phenomena which are sources of the pressures. In general the pressure field sources can be divided into 3 groups :

- The hull moving together with the secondary, surface waves system.
- Operation of the ship propeller(s).
- Vibration of the ship machines and equipment.

The developed computer system, CISAKU, makes determining the pressure field for the first and second group sources possible. The problem has been solved in a complex way, in which only the hull and propeller geometry, ship speed and propeller revolutions serve as the input data of the computation process. But all relationships within the hull-propeller system are established by the program itself. Due to this feature the CISAKU system forms a very useful tool for new ship designing. It makes possible to assess, already at the preliminary designing stage, the hull and propeller form and propeller performance parameters from the point of view of minimization of the pressure level around ship. Owing to this, construction of a ship not complying with requirements for a specified acoustic pressure level can be avoided. The program makes possible to perform a more accurate noise analysis of the existing ships a.o. by more precise identification of the acoustic sources arising from operation of ship's machines and equipment, due to elimination of the pressures induced by the hull and propeller.

The program algorithm is based on the following theoretical models :

- the velocity and pressure fields induced by the hull moving at a steady speed, are determined by means of the boundary element method (surface distribution of sources)
- the secondary wave system on the free water surface is determined by the Green function which is a solution of the Laplace equation with linear boundary conditions on the free surface
- the velocity field in the turbulent boundary layer is determined on the basis of the Karman & Leibenson integral relationships along the streamlines on the hull
- the pressure field induced by the propeller is determined by applying the model of the deformable lifting surface with elements of the twin-shell lifting surface (tip vortices).

Just these computational models are presented in more detail below.

POTENTIAL FLOW AROUND THE HULL

General assumptions of the computational model of hull potential flow can be characterized as follows :

- the hull moves forward at a steady speed on the smooth water surface
- the water region of a restricted depth, horizontally extends in all directions towards the infinity
- the sea bed is flat and parallel to the water surface

- the liquid is incompressible
- the liquid is considered inviscid outside a limited region (the boundary layer and viscous wake behind the hull)
- the flow around the hull can be described by the velocity potential $\Phi(x, y, z)$ which satisfies the Laplace equation ($\nabla^2\Phi=0$)
- the problem is considered in the Cartesian, rectangular coordinate system, 0, x, y, z, connected with the ship. 0x - axis, fixed on the hull plane of symmetry, is pointed towards the stern 0y-axis to the right side and 0z - axis vertically downwards. The system's origin is fixed on the waterplane in the mid-length between perpendiculars
- the ship moves along 0x - axis.

At the first stage of calculations the potential Φ_1 for the inviscid, incompressible liquid and inflexible water surface, in the presence of the sea bed, is searched. In terms of modelling it is equivalent to an ideal liquid flow around three, double-hull, deep-immersed models which form mirror reflections in respect to the water surface and sea bed (Fig.1).

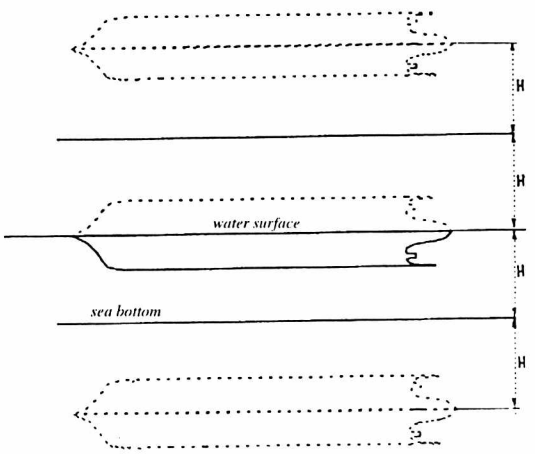

Fig.1. Schematic layout of three, double-hull models forming mirror reflections in respect to the water surface and sea bed

It was assumed that the velocity potential is generated in this case by a system of the singularities of 1/r type (Rankine source) distributed on the surfaces S of all the three double hulls :

$$\Phi_1 = \int_S \frac{q}{r} dS \tag{1}$$

Numerical solving commences from the discretization process of hull wetted surface by means of a mesh of flat quadrilateral elements (Fig.2).

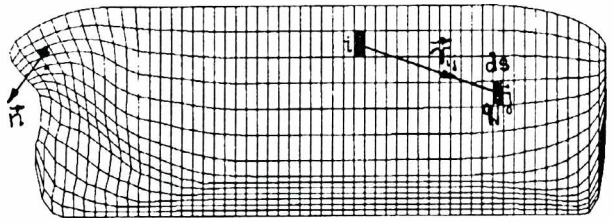

Fig.2. Scheme of the hull wetted surface discretization by a mesh of flat quadrilateral elements

The source system is determined from a set of N equations of the following form :

$$\sum_{j=1}^{N} A_{ij} q_j = \vec{n}_j \vec{V}_0 \tag{2}$$

Determination of the Aij matrix elements consists in finding the normal component of the velocities induced in the control point „i" by the unit source placed on j-th quadrilateral of the considered ship side and of its equivalents on the remaining surfaces which result from the symmetries and reflections :

$$A_{ij} = \sum_{j=1}^{N} \frac{\vec{r}_{ij}\vec{n}_j}{r_{ij}} \tag{3}$$

$$\vec{r}_{ij} = (x_i - x_j)\vec{i} + (y_i - y_j)\vec{j} + (z_i - z_j)\vec{k} \tag{4}$$

Three following cases are distinguished while calculating the coefficients A_{ij}:

- the control point „i" is placed within the quadrilateral (i=j panel), then the influence coefficient is equal to 2π
- the control point „i" is placed close to j-th quadrilateral, then the influence coefficient A_{ij} is calculated from the expressions in which the surface source distribution on j-th quadrilateral is accounted for
- the control point „i" is placed far away from j-th quadrilateral, then the influence coefficient A_{ij} is calculated from the expressions based on the assumption that all the source system is concentrated in the central point of the quadrilateral and that its intensity is equal to $Q_j=q_j dS_j$, where dS_j - quadrilateral (panel) area.

A far-away point is that distant from the panel centre by four lengths of the greater diagonal of the quadrilateral. The relevant expressions for calculating the influence coefficient A_{ij} are taken from the Hess & Smith work [5]. The set of N linear equations (2) is solved by means of the Gauss elimination method with choice of a basic element.

The solution of the set (2) makes it possible to determine the source distribution q_j on the particular hull panels. When the source system is known, the velocities $\vec{V}_i$ induced in an arbitrary point of the space surrounding the hull and also on the hull itself can be determined.

The pressure p in the space around the hulls is calculated by using the Bernoulli equation :

$$p - p_\infty = \frac{1}{2}\left[V_0^2 - \left(\vec{V}_0 - \vec{V}_i\right)^2\right] \tag{5}$$

At the second stage of calculations the velocity potential Φ_2 connected with restoring the water surface flexibility is determined. The solutions of the Green function for the point pressure impulse moving with a steady speed [6] are used in the computational model. The mathematical description of the problem for a single point pressure impulse is the following [4,13,14].

The velocity potential φ satisfies the Laplace equation with the linear boundary conditions on the free water surface :

$$\frac{\partial^2\varphi}{\partial x^2} - \frac{g}{V_0}\frac{\partial\varphi}{\partial z} - \frac{\mu}{V_0}\frac{\partial\varphi}{\partial x} = \frac{1}{\rho V_0}\frac{\partial p_c}{\partial x} - \frac{1}{\rho}\nabla p_c \nabla\varphi \tag{6}$$

$$\zeta(x,y) = -\frac{V_0}{g}\frac{\partial\varphi}{\partial x} + \frac{p_c}{\rho g} \tag{7}$$

The searched solution for the potential of the single point pressure impulse $p_0 = p_c\partial(x)\partial(y)$ is obtained by applying the Fourier transformation [13,14] and assuming $\nabla p_c \nabla\varphi$ to be a negligible value :

$$\varphi(x,y,z) = -\frac{ip_0}{4\pi^2\rho V_0}\int_{-\pi}^{\pi}\sec\theta d\theta\int_0^{\infty}\frac{e^{-kz}e^{ik(x\cos\theta+y\sin\theta)}dk}{k - k_0\sec^2\theta + i\frac{\mu}{V_0}\sec\theta} \tag{8}$$

Here and in (9) : $i = \sqrt{-1}$

The free water surface deformation is obtained by using (7) :

$$\zeta(x,y) = -\frac{p_0}{4\pi^2 \rho g} \int_{-\pi}^{\pi} d\theta \int_0^{\infty} \frac{e^{ik(x\cos\theta + y\sin\theta)} k^2 dk}{k - k_0 \sec^2\theta + i\frac{\mu}{V_0}\sec\theta} \tag{9}$$

A form of the expression (9) suitable for numerical calculations is achieved by performing the further transformations [4] :

$$\zeta(x,y) = -\frac{p_0}{2\pi^2 \rho g} \int_0^{\pi/2} \cos^4\theta \, d\theta \int_0^{\infty} \frac{k^3 (e^{-k|Z_1|} + e^{-k|Z_2|})}{k^2 \cos^4\theta + k_0^2} dk + \tag{10}$$

$$+ \frac{p_0}{\pi\rho g} \int_0^{\pi/2} \frac{k_o^2}{\cos^4\theta} \left[H(Z_1) \sin\left(\frac{k_0 Z_1}{\cos^2\theta}\right) + H(Z_2) \sin\left(\frac{k_0 Z_2}{\cos^2\theta}\right) \right] d\theta$$

where :

$$\begin{aligned} Z_1 &= x\cos\theta + y\sin\theta \\ Z_2 &= x\cos\theta - y\sin\theta \end{aligned} \tag{11}$$

$$\begin{aligned} H(Z_1) &= 0 \quad if \;\; Z_1 \geq 0 \qquad H(Z_1) = 1 \quad if \;\; Z_1 < 0 \\ H(Z_2) &= 0 \quad if \;\; Z_2 \geq 0 \qquad H(Z_2) = 1 \quad if \;\; Z_2 < 0 \end{aligned} \tag{12}$$

By applying a modification to eliminate high wave amplitudes the searched solution for the height of the wave generated by a single point pressure impulse moving with an arbitrary steady speed was obtained [7]. The universal tables of data were prepared by introducing the normalized magnitudes (the wave height in an arbitrary point was related to the wave height in the impulse position point, and the coordinates x, y were related to the wave number k_0), which make it possible to find, in a short time by means of interpolation, the wave system generated by an arbitrary pressure impulse moving at an arbitrary steady speed. The wave system generated by the single pressure impulse is illustrated in Fig.3.

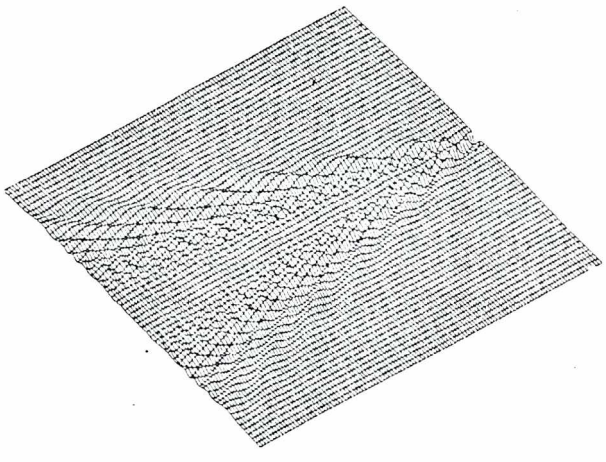

Fig.3. The wave system generated by the point pressure impulse

The so-called Bernoulli wave is the starting point for calculations of the wave system generated by the hull moving at a steady speed. At the first stage it is obtained from the calculated pressure field on the inflexible water surface. Releasing the surface provides a distinct image of the pressure field just in the form of the Bernoulli wave. Its motion along with the hull generates the secondary wave system.

In the assumed computational model a streamline-based mesh is formed on the water surface around the hull. The point pressure impulse P_0 is determined in the centre of the mesh element :

$$p_0 = \iint_{S_c} p dS \tag{13}$$

Each of the impulses generates its own wave system. The superposition of the waves generated by the impulse system gives a resultant wave generated by the hull on the water surface. Such wave system generated by the Wigley's model of the block coefficient C_B=0.44 at the Froude number F_n = 0.316 is presented in Fig.4.

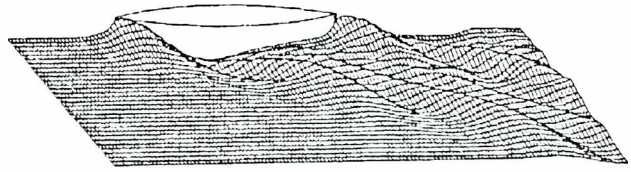

Fig.4. The wave system generated by Wigley's model

When the resultant wave height is known the x - component of the velocity on the water surface is determined by means of the expression resulting from the boundary condition (7) :

$$V_{fx} = \frac{\partial \Phi_2}{\partial x} = -\frac{g}{V_0}\zeta \tag{14}$$

The potential Φ_2 is the superposition of the potentials φ of all the point pressure impulses on the water surface. It is not necessary to know the potential Φ_2 any further. However it is necessary to know the velocities induced by the system in an arbitrary point under water. It was assumed according to the surface wave theory that the velocities vary exponentially, in compliance with the formula :

$$e^{-\frac{gz}{V_0^2}}$$

under the condition that the values of the depth z and position of the points under the water surface are determined with the use of the stream surfaces formed around the hull. It means that the ship hull does not project "shadows" onto the planes beneath it, but the wave system on the water surface is entirely transformed beginning from the hull plane of symmetry.

To account for the sea-bed effect the potential Φ_2 is required to be composed of two wave systems: a part equivalent to the actual water surface and part being its mirror reflection in respect to the sea bed surface (Fig.5). In this case the velocities induced by the wave system generated on the water surface will be determined by means of two segments differring with the depth z (in respect to an actual surface and that mirror-reflected).

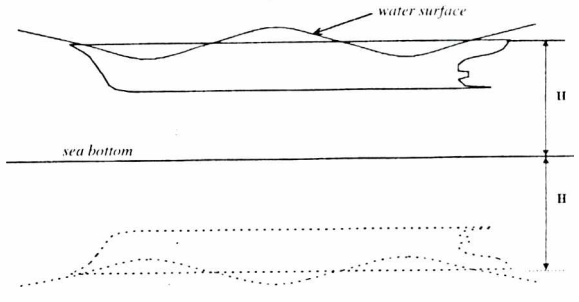

Fig.5. Schematic layout of the model on the waving water surface, forming mirror reflection respective to the sea bed surface

The calculated velocities induced by the secondary wave system make it possible to calculate the potential flow pressure field. These calculations complete the second stage of works on the computational model of the potential flow around the hull.

VISCOUS FLOW AROUND THE HULL

Calculations of the turbulent boundary layer on the basis of the average Navier-Stokes equation were withdrawn from consideration

in result of the analysis of the existing computational models of viscous liquid flow around the hull. First of all the reason was that an exact computational model of the viscous flow around the hull itself is not required for determining the pressure field around it. An effective (optimal) computational model was selected, based on the determination of boundary layer parameters along hull streamlines, and the model itself based on the integral relationships which concern the boundary layer of Karman [16] :

$$\frac{d}{dx'}(\delta_2)+\frac{1}{U}\frac{\partial U}{\partial x'}(2\delta_2+\delta_1)=\frac{\tau_0}{\rho U^2} \tag{15}$$

and that of Leibenson :

$$\frac{d}{dx'}(U^3\delta_3)=2\nu\int_0^{\delta}\left(\frac{du}{dy'}\right)^2 dy \tag{16}$$

The flow around the hull is approached, by proceeding the calculations along the streamlines, to the two-dimensional flow, i.e. to the case in which the above stated relationships are valid.

Basic expressions of the computational algorithm were elaborated in compliance with the Poilin Xian's work [15]. Results are obtained by solving the system of two ordinary, first-order differential equations, with the use of the Runge-Kutta method :

$$\frac{d\delta_2}{dx'}=-(H_{12}+2)\frac{\delta_2}{U}\frac{du}{dx'}+\frac{1}{2}U^2C_f \tag{17}$$

$$\frac{dH_{32}}{dx'}=(H_{12}-1)H_{32}\frac{1}{U}\frac{dU}{dx'}+\frac{0.0112}{\left(\frac{U\delta_2}{\nu}\right)^{1/6}\delta_2}-\frac{1}{2}U^2C_fH_{32} \tag{18}$$

$$C_f=\frac{1}{\frac{1}{2}U^2}\frac{0.123\cdot 10^{-0.678H_{12}}}{\left(\frac{U\delta_2}{\nu}\right)^{0.268}} \tag{19}$$

When δ_2 and H_{32} are known it is possible to calculate the remaining parameters of the boundary layer by means of the known relationships of the single parameter description of the boundary layer :

$$w_n=\frac{4-3H_{32}}{H_{32}-2} \tag{20}$$

$$\delta=\frac{\delta_2(w_n+1)(w_n+2)}{w_n} \tag{21}$$

$$\delta_1=\frac{\delta}{w_n+1} \tag{22}$$

$$\delta_3=\frac{2w_n\delta}{(w_n+1)(w_n+3)} \tag{23}$$

$$H_{12}=\frac{\delta_1}{\delta_2}=\frac{w_n+2}{w_n} \tag{24}$$

$$H_{32}=\frac{\delta_3}{\delta_2}=\frac{2(w_n+2)}{w_n+3} \tag{25}$$

Calculation results of the hull boundary layer are used in the program in two ways.

Firstly, the displacement thickness of the boundary layer is determined, based on the flow intensity of the liquid contained within the boundary layer, and the hull form is extended by the thickness. The calculations performed at the stage I are repeated with the use of such modified hull form. They are completed when values of the flow parameters are obtained in two consecutive steps with an assumed accuracy.

Secondly, the velocity field of the boundary layer, at the end of the hull serves to calculating the velocity field in the area of propeller operation. A computational model of the flow behind the hull is presented in the next section.

VELOCITY FIELD IN THE PROPELLER DISC

A starting point for the calculations of the velocity field in the propeller disc is the velocity field induced by the hull itself and the velocity field of the boundary layer at the end of the hull. The calculations can be carried out without the propeller (nominal field) or with the propeller accounted for (effective field). In the latter case the propeller-induced velocity field is also accounted for in the calculations of the velocity field in the propeller disc (however the induced velocities are not taken into account in the velocity field at the propeller disc itself).

At the beginning the zero starting points of the streamlines that cross the propeller disc are assumed on the hull ends (up to 15 in number). The number of the starting points can be increased by assuming, within the boundary layer, from the zero point along the normal line in respect to the hull, 9 points with determined values of the ratio of the local velocity to that on the boundary layer limit.

Then the transformation of the boundary layer velocity field is performed. Namely, the velocity profile in the layer on the hull surface is characterized by a single parameter distribution described by the following expression :

$$\frac{u}{U}=\left(\frac{y}{\delta}\right)^{w_n} \tag{26}$$

But the velocity field in the viscous wake behind the hull is characterized by the universal distribution typical of the fully formed flow with the turbulent exchange of momentum :

$$\frac{1-\frac{u}{U}}{1-\frac{U_n}{U}}=\left(1-\left(\frac{y}{\delta}\right)^{3/2}\right)^{w_{n2}} \tag{27}$$

The velocity profiles in the boundary layer and in the wake behind it are shown in Fig.6.

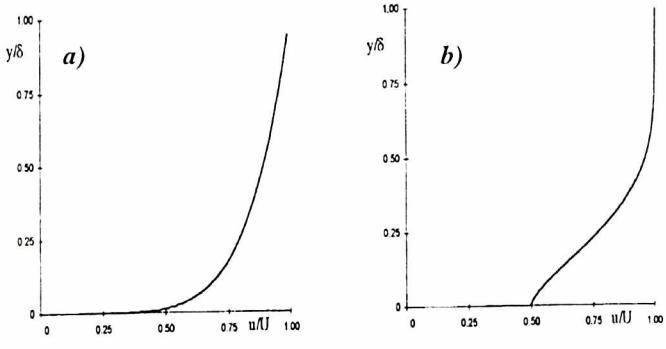

Fig.6. The velocity profiles:
a) in the boundary layer; b) in the flow with the turbulent momentum exchange

The transformation consists in determining the exponent w_{n2} and the velocity U_n with the assumed momentum constant in both flows [11].

In the presented calculation version, values of the exponent w_n and w_{n2} are assumed equal and only U_n value has to be determined. In result of appropriate transformations the following expression is yielded :

$$U_n = \frac{\frac{1.38}{w_n^2} - 1.67}{w_n} + 0.7696 \tag{28}$$

It is next assumed that the flow expands in compliance with the turbulent flow theory and the velocity U_n changes in accordance to the following relationship :

$$U_n = 1.0 - \frac{1 - U_{n0}}{\sqrt{1 + 0.97s}} \tag{29}$$

On such defined velocity profile in the boundary layer the points of the determined u/U values are established .Nine values were selected and they formed starting points for the streamlines whose trajectories were further determined on the basis of the hull-induced velocity field and , if necessary, of that induced by the propeller.

The traces of the particular streamlines on the propeller disc plane make determining the velocities at that plane possible.

In the case of calculation with the propeller, the effective wake coefficient w_e is obtained from the approximate formulae (using the hull form data) in order to decrease the number of calculation steps. Basing on the average velocity field at the propeller disc the propeller-induced velocities are calculated and the propeller-induced velocities $\vec{V}_{\gamma i}$ at the check points on the hull are determined already in the first calculation step. The velocities are included in the boundary condition and therefore the equation set (2) gets the following form :

$$\sum_{j=1}^{N} A_{ij} q_j = \vec{n}_j \left(\vec{V}_0 + \vec{V}_{\gamma i} \right) \tag{30}$$

In further calculation steps the velocity field at the propeller disc is used, determined in line with the above presented scheme.

COMPUTATIONAL MODEL OF THE PROPELLER

The propeller has a very important role in the presented program. It influences, directly and indirectly, the hydrodynamic pressure field around the hull as well as it is itself the most important source of acoustic pressures, especially in the case of the cavitating propellers.

Therefore the computational model of the propeller is based on the well verified theoretical model of the deformable lifting surface [17].

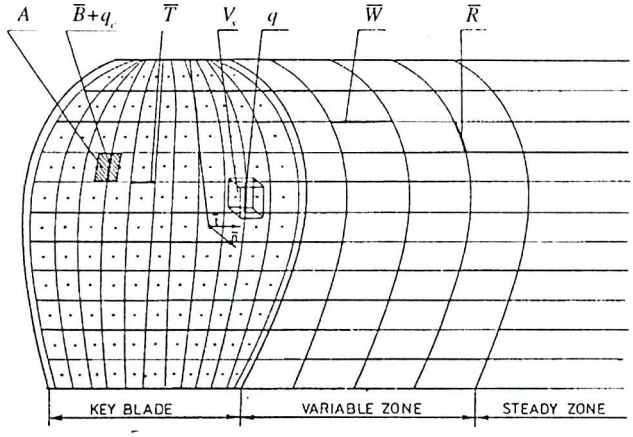

Fig.7. Discrete vortex/source model of the propeller blade

The computational model is based on the discrete mesh of the vortex and source singularities. On each propeller blade 165 elements of the bound vortices **B** are placed which model the hydrodynamic load distribution on the lifting surface (Fig.7).

Each of the elements represent the vorticity concentrated on the surface ΔS. To be in compliance with the Kelvin principle on the vorticity conservation, the bound vortices should be supplemented by the set of 168 elements of the bound vortices **T**. The intensity of **T**-elements can be expressed by a linear combination of the intensities of **B**-elements located on the lifting surface strips neighbouring on each other.

Behind the blade trailing edge the helix surfaces are formed from the elements of the free vortices **W** which are extensions of the trailing vortices **T**. The part of the free vortex system, closest to the trailing edge, forms the variable zone of the free vortex system in which the radius -oriented vortex elements **R** exist additionally. The remaining part of the system forms the steady zone consisting of the elements **W** only. The variable zone influences, by the induced velocities, an actual kinetic situation on the blade. The blade thickness as well as the sheet cavity thickness is modelled by means of the sources and sinks discrete distribution q. The classical linearization assumption is applied dealing with the separation of the hydrodynamic loading effect from the thickness effect.

The key point of the method is the kinematic boundary condition on the lifting surface which requires the resultant relative velocity of flow to be tangent to the surface. It leads to the following integral equation :

$$\frac{1}{4}\left[\iint_{S_c} \vec{n}\gamma\nabla\left(-\frac{1}{r_p}\right)dS + \iint_{S_p} q\frac{\partial}{\partial n}\left(-\frac{1}{r_p}\right)dS \right] + \left(\vec{V}_0 + \vec{\omega}\cdot\vec{r}\right)\vec{n} = 0 \tag{31}$$

where :

$$\gamma = \gamma_p + \gamma_{pv}$$
$$q = q_p + q_c$$

By solving the equation numerically system of a linear equation is obtained, however in order to complete the system the Kutta condition on the trailing edge is used additionally.

The linear equation system is solved by applying the Gauss-Jordan elimination method with the basic element selection.

When the intensities of the vortex elements **B**, **T**, **W** and **R** are already determined it is possible to determine the induced velocities on the lifting surface, as well as those at an arbitrary point of space surrounding the propeller. The Biot-Savart expression is applied to calculate the induced velocities.

The computational model of the propeller applied in the program is suitable for analyzing the propeller operation in the non-uniform velocity field behind the hull, with possible cavitation detection and determination of the acoustic pressures induced by it.

The pressures on propeller blades are evaluated on the basis of the Bernoulli unsteady flow equation :

$$C_p = \frac{p - p_\infty}{\frac{1}{2}\rho V_0^2} = 1 - \left(\frac{V_p}{V_\infty}\right)^2 - \frac{2}{V_0^2}\frac{\partial \Phi_s}{\partial t} \tag{32}$$

In practice the segment $\frac{\partial \Phi_s}{\partial t}$ of the equation (32) is substituted by the finite difference of the values obtained from the analysis of the separate blade positions in the non-uniform velocity field.

Three different forms of cavitation, shown in Fig.8, can be distinguished and modelled :

- sheet (laminar) cavitation
- bubble cavitation
- tip vortex cavitation.

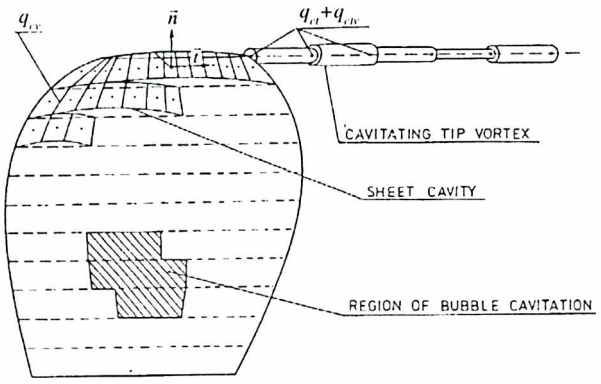

Fig.8. Model of the cavitation phenomena on the propeller blade

Detection of the sheet and bubble cavitation inception is based on the behaviour analysis of the vapour-filled micro-bubbles present in the water, which act as the cavitation nuclei in the variable pressure field on the blade surface. The Rayleigh-Plesset equation which describes the dynamics of an isolated, spherical, vapour-filled bubble [6] is the basis for the analysis :

$$\frac{d^2R_b}{dt^2} = \left[\frac{\Delta p}{\rho} - \frac{3}{2}\left(\frac{dR_b}{dt}\right)^2 - \frac{2S_x}{\rho R_b} - \frac{4\mu}{\rho R_b}\frac{dR_b}{dt}\right]\frac{1}{R_b} \qquad (33)$$

The equation (33) is solved step-wise for each analyzed blade section by means of the Runge-Kutta method. It is solved for the initial conditions $R_b = R_{b0}$ and $dR_b/dt = 0$, where R_{b0} is the average radius of bubbles in the inflow. The cavitation inception is assumed when the actual radius of the bubble exceeds the prescribed critical value R_c . If it happens within 5% range of the blade chord length from the leading edge, the inception of sheet cavitation is assumed to occur, otherwise the bubble cavitation is assumed to commence. The region covered by the bubble cavitation extends to the point where the local pressure value on the blade exceeds the critical value.

It is assumed that the dynamic changes of the sheet cavity geometry can be modelled by an additional, discrete system of sources q_{cv} distributed on the part of the lifting surface, actually covered by the cavity. The intensity of sources q_{cv} can be obtained from the dynamic boundary condition on the sheet cavity surface :

$$\frac{1}{2\pi V_0^2}\iint_{S_k}\frac{dq_{cv}}{dt}\frac{\partial}{\partial n}\left(-\frac{1}{r_p}\right) = C_p - \sigma_0 - \frac{4S_c}{\rho V_0^2 R_c} \qquad (34)$$

The condition forms the linear equation system whose solution makes it possible to determine an increase of the sheet cavity thickness in the time interval between two consecutive analyzed angular positions of the propeller blade. The so-defined sheet cavity introduces a deformation of the initial lifting surface form, which influences the kinematic boundary condition at the consecutive analyzed angular position of the blade. The instantaneous cavity thickness is modelled by means of the discrete system of sources q_c .

Detection of the cavitating tip vortex is performed on the basis of the model where the vorticity is assumed concentrated inside the vortex core of a known radial distribution of vorticity. Outside the core the flow is assumed irrotational. As the instantaneous streamlines of the free vortex system are in line with the vortex lines, determining the pressure around the vortex as well as that inside the vortex core is possible. The core internal pressure must fall low enough to cause growing the cavitation nuclei above the critical size. This is analyzed again by means of the equation (33).

The tip vortex, due to its variable intensity during the propeller operation in the non-uniform velocity field, is modelled by a series of the vortex segments of different cavitating core diameters.

The variable pressure field generated by the cavitating propeller is determined on the basis of the linearized form of the Bernoulli equation of unsteady flow :

$$\Delta p(t) = \rho\left(\frac{\partial \Phi_p}{\partial x}V_0 - \frac{\partial \Phi_p}{\partial t}\right) \qquad (35)$$

The potential Φ_p in (35) contains the contributions from all the singularities modelling the propeller, the free vortex system as well as the sheet and tip vortex cavitations. The potential Φ for the vortex surfaces is determined by means of an equivalent dipole distribution. Every quadrilateral formed by the vortices on the lifting surface and free vortex system is substituted by a relevant single dipole located at the centre of the quadrilateral.

After performing the calculations for all analyzed blade positions during one propeller rotation, the harmonic analysis is carried out of the instantaneous pressure values and the values of particular spectral lines of the discrete spectrum of the variable pressure field generated by the propeller are obtained.

FINAL REMARKS

On the basis of the presented theoretical models the appropriate computational algorithms of the program for determining the pressure field around the hull moving at steady speed and the cooperating propeller, in the conditions of restricted water depth, were elaborated.The CISAKU system with a suitable graphic sub-program was put into operation. Some results of calculations and their analysis will be presented in the paper „Computer software system for determining the pressure field resulting from hull flow and operation of the marine propeller".

NOMENCLATURE

- A - propeller blade area element
- A_{ij} - matrix elements
- B - bound vortex elements
- C_f - local friction coefficient
- C_p - pressure coefficient
- F_n - Froude number $F_n = \frac{V_0}{\sqrt{gL_c}}$
- g - acceleration of gravity
- H - water depth
- H_{12} , H_{32} - boundary layer parameters of its single-parameter description
- k - wave vector coordinate in the polar coordinate system
- k_0 - wave number $k_0 = g/V_0^2$
- L_c - hull length on the waterline
- $\vec{n}$ - vector normal to the surface
- $\vec{n}_j$ - vector normal to the surface in j-th point
- p - pressure
- p_c - pressure on the water surface
- p_0 - point pressure impulse
- p_∞ - undisturbed flow pressure
- q - source intensity
- q_j - source intensity on j-th element
- q_p - source intensity modelling the blade thickness
- q_c - source intensity modelling the cavities
- q_{cv} - source intensity modelling the sheet cavity thickness
- q_{ct} - source intensity modelling the tip vortex cavitation core
- q_{ctv} - source modelling the dynamics of the cavitating tip vortex
- Q_j - concentrated source intensity on j-th hull element
- r - radius - vector
- r_{ij} - distance between i-th and j-th points
- r_p - distance between the control point and vortex element (or source) location
- R - free vortex elements which account for unsteady conditions on the propeller blade
- R_b - gas bubble radius
- R_c - chordwise curvature radius of the sheet cavity
- s - streamline-wise coordinate
- S_c - area of the vortex surface comprising both bound and free vortex system
- S_k - area of laminar cavity surface
- S_c - area of water surface element
- S_p - propeller blade area
- S_x - water surface tension
- t - time
- $\vec{t}$ - tangetial vector
- T - bound vortex elements on the propeller blade, chordwise directed
- u - local velocity in the viscous wake
- U - velocity at the viscous wake boundary
- U_n - velocity in the middle of the viscous wake
- U_{n0} - velocity in the middle of the viscous wake at its starting point
- V_0 - hull speed
- $\vec{V}_i$ - flow velocity induced by the hydrodynamic singularities

$\vec{V}_{\gamma i}$ - flow velocities induced by the propeller
V_{ix} - x-wise velocity components on the water surface, induced by the secondary wave system
V_p - resultant velocity at the control point
V_i - propeller blade volume element
w_e - effective wake coefficient
w_{n1}, w_{n2} - exponents appearing in the formulae for velocity distribution in the boundary layer and viscous wake, respectively
W - free vortex elements
x, y, z - rectangular coordinates of the reference system connected with the hull
x', y' - rectangular coordinates of the movable reference system connected with the streamlines on the hull
z - depth of a point under water surface
γ - vortex element intensity
γ_p - vortex element intensity on the lifting surface
γ_{fw} - vortex element intensity of the free vortex system
δ - boundary layer thickness
δ_1 - flow rate loss thickness
δ_2 - momentum loss thickness
δ_3 - energy loss thickness
$\delta(x),\delta(y)$ - dimensions of the water surface rectangular element used to determining the pressure impulse
ζ - wave height of the secondary wave system on the water surface
θ - wave vector coordinate in the polar reference system
μ - dynamic viscosity coefficient
ν - kinematic viscosity coefficient
ρ - liquid density
σ_n - cavitation number
τ_n - tangent stresses on the panel
φ - velocity potential of the secondary, single-pressure-impulse-generated wave system
Φ - velocity potential which totally describes flow around the hull
Φ_2 - velocity potential connected with the secondary, hull-generated wave system
Φ_p - velocity potential effected by all the singularities modelling the propeller, free vortices and cavitation
Φ_s - velocity potential which expresses propeller blade operation
ω - angular velocity.

BIBLIOGRAPHY

1. Bugalski T., Koronowicz T., Szantyr J., Waberska G.: „System komputerowy do wyznaczania opływu statku wraz z układem falowym". Materiały X Sympozjum Hydromechaniki Okrętowej, Gdańsk, 1993
2. Bugalski T., Koronowicz T., Szantyr J., Waberska G.: „Computer System for Calculation of Flow, Resistance and Propulsion of a Ship at the Design Stage". CADMO '94, Southampton, 1994
3. Bugalski T., Koronowicz T., Szantyr J., Waberska G.: „A Method for Calculation of Flow Around the Hull of a Ship Moving in Calm Water with Constant Velocity". Marine Technology Transactions, 1994, vol. 5
4. Grygorowicz M., Rogalski A.: „Badanie numeryczne funkcji opisującej fale generowane na swobodnej powierzchni przez impuls ciśnienia". Materiały X Konferencji Mechaniki Płynów, Gdańsk - Sarnówek, 1992
5. Hess J.L., Smith A.M.O.,: „Calculation of Potential Flow About Arbitrary Bodies". Progress in Aeronautical Sciences, vol. 8, Pergamon Pres, Oxford, 1966
6. Knapp R.T., Daily J.W., Hammitt F.G.: „Cavitation". Mc Graw-Hill, New York, 1970
7. Koronowicz T.: „Numeryczne rozwiązanie formuły opisującej fale generowane przez impuls ciśnienia na swobodnej powierzchni wody". Zeszyty Naukowe IMP PAN, nr 427/134/84
8. Koronowicz T.: „Kawitacja wirowa źródłem wysokiego poziomu ciśnień akustycznych od śrub okrętowych". Materiały XI Sympozjum Hydroakustyki, Gdynia-Jurata, Maj 1994
9. Koronowicz T.: „Model wirowy dwupowłokowej powierzchni nośnej". Materiały XI Krajowej Konferencji Mechaniki Płynów, Warszawa, 1994
10. Koronowicz T., Szantyr J.: „A New Theoretical Model of Formation of Vortex Cavitation". Proceedings of PROPCAV '95 International Conference on Propeller Cavitation, Newcastle upon Tyne, 1995
11. Koronowicz T., Grabowska K.: „Propozycja wyznaczania pola prędkości w kręgu roboczym śruby". Raport IMP PAN, nr arch. 274/97
12. Kozaczka E.: „Szumy podwodne wytwarzane przez statki w morzu płytkim". Materiały XI Sympozjum Hydroakustyki, Gdynia-Jurata, Maj 1994
13. Krężelewski M.: „Hydromechanika ogólna i okrętowa". Cz. II, Wyd. Politechniki Gdańskiej, Gdańsk, 1982
14. Krężelewski M., Rogalski A.: „Numeryczne wyznaczanie obrazu fal generowanych przez impuls ciśnień". Materiały X Sympozjum Hydromechaniki Okrętowej, 1993
15. Peilin Xian: „Strommungsmechanische Untersuchung der Zustromduse". Praca doktorska, Wyd. Rheinisch-Westfalische Technische Hochschule, Aachen, Marz 1989
16. Prosnak W.J.: „Mechanika płynów". PWN, Warszawa, 1970
17. Szantyr J.A.: „A Method for Analysis of Cavitating Marine Propellers in Non-uniform Flow". International Shipbuilding Progress, Vol. 41, September 1994.

Current reports

POLISH NAVAL ACADEMY GDYNIA
INSTITUTE OF SHIP TECHNICAL MAINTENANCE

A new version of analyzer for engine measurements and diagnostics

Pressure analyzers, called also MIP calculators, are the most frequently installed on ships measurment - diagnostic instruments used to controlling the fuel combustion and injection processes and regulating the ship engines. AUTRONICA analyzers are examples of the devices.

Several versions of the analyzer for measuring and indicating the maximum combustion pressure, mean indicated pressure, maximum compression pressure and self-ignition angle were elaborated by the Institute of Ship Technical Maintenance, Polish Naval Academy in Gdynia. Moreover, measuring the vibration acceleration envelope was also added to their design, which is not the case of other analyzer constructions. EAD-MA2 analyzer is the new elaborated version with high measuring abilities. The basic transducer card ensures the conversion with 1 MHz/12 b frequency in the case of single channel operation. The sampling angular resolution of 0.1° of crankshaft rotation was applied which provides many additional measurement possibilities.

When elaborating the new version a further progress was achieved in processing and presenting the parameters of the developed indicator diagram a.o., by introducing the colour imaging and a programming procedure for minimizing the measuring error of MIP (p_i) determination, and by applying a special procedure for the inner-dead-centre determination. Moreover the function of generating the first derivative dp/da within the crankshaft rotation angle domain was applied, but the analyzer is able to generate derivatives and integrals of any order. For that a special spline method of the follow-up approximation was developed. Knowledge of dp/da course is very useful for determining the self-ignition starting point of the high-load, medium- and high-speed engines.

EAD-MA2 analyzer, equipped with 17" SVGA monitor, trackball operation and Windows environment, was already installed on a 150 000 t bulk carrier. It can be operated keyboard-less. Starts and stoppages of the engine and other dynamic processes can be also recorded due to the application of an additional card which makes recording the fast changeable courses (of cylinder pressures, vibrations) possible.

A combustion pressure transducer and acceleration transducer was installed on each cylinder of the engine of the above mentioned ship as well as of engines of all ships equipped with EAD-MA1 analyzer. The signals emitted by two inductive gauges: the first one triggered by the turning gear teeth, and the second by the engine flywheel, are used to control the inner dead centre and generate the angle axis.

EAD-MA2 analyzer can also operate as a portable device.